

## Original Article

## Physicochemical properties and photocatalytic activity of bismuth oxide as affected by weak or strong base precipitants

Yayuk Astuti<sup>1\*</sup>, Arum Dista Wulansari<sup>1</sup>, Abdul Haris<sup>1</sup>,  
Adi Darmawan<sup>1</sup>, and Ratna Balgis<sup>2</sup><sup>1</sup> Department of Chemistry, Faculty of Science and Mathematics,  
Diponegoro University, Semarang, Central Java, 50275 Indonesia<sup>2</sup> Department of Chemical Engineering, Graduate School of Engineering,  
Hiroshima University, Hiroshima, 7398511 Japan

Received: 27 October 2018; Revised: 8 April 2020; Accepted: 22 April 2020

**Abstract**

The role of the precipitating agent on the formation of bismuth oxide was carefully evaluated. This research aims to investigate the influence of choice of strong or weak bases as the precipitating agent on the physicochemical properties of bismuth oxide, as regards crystal structure, morphology, bandgap, and photocatalytic activity. Bismuth oxide particles synthesized using  $\text{NH}_4\text{OH}$  as the precipitating agent had the form of bright yellow powder with  $\alpha$  and  $\beta$  crystal structures, 0.6-5.2  $\mu\text{m}$  size, and bandgaps of 2.51 and 2.88 eV, respectively; while bismuth oxide synthesized using  $\text{NaOH}$  as the precipitating agent was a pale yellow powder with  $\alpha$ ,  $\beta$  and  $\delta$  crystal structures, 2.50-10  $\mu\text{m}$  in size, and bandgap of 2.80 eV. The amounts of OH and NO functional groups as impurities in the particles was decreased by calcination. Furthermore, the photocatalytic activity of  $\text{Bi}_2\text{O}_3$  was better than that of  $\text{BO}_4$  with reaction rate constants  $2.38 \times 10^{-3} \text{ s}^{-1}$  and  $0.68 \times 10^{-5} \text{ s}^{-1}$ , respectively, probably because of the different physicochemical properties.

**Keywords:** bismuth oxide, precipitation method, precipitating agent, photocatalyst**1. Introduction**

Bismuth oxide ( $\text{Bi}_2\text{O}_3$ ) is a pale yellow metal oxide having a melting point of 825°C that is insoluble in water. Bismuth oxide has six types of polymorphs, namely  $\alpha$ - $\text{Bi}_2\text{O}_3$  (monoclinic),  $\beta$ - $\text{Bi}_2\text{O}_3$  (tetragonal),  $\gamma$ - $\text{Bi}_2\text{O}_3$  (body centered cubic),  $\delta$ - $\text{Bi}_2\text{O}_3$  (face centered cubic),  $\varepsilon$ - $\text{Bi}_2\text{O}_3$  (orthorhombic) and  $\omega$ - $\text{Bi}_2\text{O}_3$  (triclinic). The formation of  $\alpha$ - $\text{Bi}_2\text{O}_3$  takes place at a temperature of 400 °C;  $\alpha$ - $\text{Bi}_2\text{O}_3$  converts to  $\delta$ - $\text{Bi}_2\text{O}_3$  at a temperature of 729 °C. The formation of  $\beta$ - $\text{Bi}_2\text{O}_3$  occurs at temperatures from 400 °C to 729 °C;  $\beta$ - $\text{Bi}_2\text{O}_3$  polymorph is metastable at high temperatures. Furthermore,  $\gamma$ - $\text{Bi}_2\text{O}_3$  polymorph is metastable at high temperatures; meanwhile, the formation of  $\delta$ - $\text{Bi}_2\text{O}_3$  takes place at a temperature of 750 °C.

The polymorph  $\delta$ - $\text{Bi}_2\text{O}_3$  changes to  $\beta$ - $\text{Bi}_2\text{O}_3$  at 650 °C, while  $\delta$ - $\text{Bi}_2\text{O}_3$  changes to  $\gamma$ - $\text{Bi}_2\text{O}_3$  at 639°C (Mallahi, Shokuhfar, Vaezi, Esmaeilrad, & Mazinani, 2014). It also has a high oxide ion mobility with potential applications in fuel cell (Boivin, 2001), gas sensing (Sammes, Tompsett, Näfe, & Aldinger, 1999), electrolyzers (Goodenough, 2003), ceramic membranes for high purity oxygen separation (Kharton, Naumovich, Yaremchenko, & Marques, 2001), partial oxidation of hydrocarbons (Switzer, Shumsky, & Bohannan, 1999) and photocatalysis (Astuti *et al.*, 2016, 2017).

The physicochemical properties of a material determines its application performance. It is widely known that the physicochemical properties, such as crystal structure (Cao, 2004), morphology, and photocatalytic activity (Serpone & Pelizzetti, 1989), are affected by the synthesis method. Therefore, several methods have been developed to synthesize  $\text{Bi}_2\text{O}_3$ , including precipitation (Astuti *et al.*, 2017), combustion (Aruna & Mukasyan, 2008; Astuti *et al.*, 2016; La

\*Corresponding author

Email address: yayuk.astuti@live.undip.ac.id

*et al.*, 2013), hydrothermal (Wu, Shen, Huang, & Zhang, 2011), and sol gel (Mallahi *et al.*, 2014) approaches. Among these, precipitation has the most advantages, such as simplicity of the process, easily obtained reagents and tools, easy control of particle size, and that the time required is relatively short. Several factors, such as reactants, temperature, and mixing process determine the crystal formation of the precipitation products (Skoog, West, Holler, & Crouch, 2013). For example, n-ZnO was transformed from plate-like morphology with 3.44 eV bandgap into p-ZnO with flower type morphology and 3.37 eV bandgap by changing the precipitating agent from  $\text{NH}_4\text{OH}$  to NaOH.

Bismuth oxide was successfully synthesized by precipitation, by Astuti and colleagues, from bismuth oxynitrate ( $\text{Bi}_5\text{O}(\text{OH})_9(\text{NO}_3)_4$ ) as the precursor. It was found that the photocatalytic properties were better when  $\text{NH}_4\text{OH}$  was used as precipitating agent than when using NaOH (Yayuk Astuti *et al.*, 2017).

It is well known that bismuth (III) nitrate pentahydrate ( $\text{Bi}(\text{NO}_3)_3 \cdot 5\text{H}_2\text{O}$ ) is commonly used as the precursor in synthesis of bismuth oxide. However, to the best of the author's knowledge, several studies of bismuth oxide synthesis with  $\text{Bi}(\text{NO}_3)_3 \cdot 5\text{H}_2\text{O}$  as a precursor used  $\text{NH}_4\text{OH}$  as the precipitating agent, without considering the effect of using alternative precipitating agents (Astuti, Ningsih, Arneli, & Darmawan, 2018; Bartonickova, Cihlar, & Castkova, 2007; Hwang *et al.*, 2009; Li, 2006; Patil, Deshpande, Dhage, & Ravi, 2005; Stewart *et al.*, 2016). In addition, the investigation of effects on physicochemical properties by the precipitating agent used in synthesis is little explored. Therefore, in this research, bismuth oxide synthesis by precipitation was performed testing strong and weak bases as alternative precipitating agents. This is related to the alkalinity of the precipitating agent, namely  $\text{NH}_4\text{OH}$  or NaOH as weak or strong base, respectively. When  $\text{NH}_4\text{OH}$  is dissolved in water, it is not completely dissociated to  $\text{NH}_4^+$  and  $\text{OH}^-$  ions; in contrast, NaOH dissociates to  $\text{Na}^+$  and  $\text{OH}^-$  ions perfectly when dispersed in water. The strong base NaOH generates more  $\text{OH}^-$  ions because it is perfectly ionized in water, while the weak base  $\text{NH}_4\text{OH}$  produces fewer  $\text{OH}^-$  ions due to only partial dissociation. Therefore, on precipitating  $\text{Bi}^{3+}$  ions, NaOH as the precipitating agent is faster than  $\text{NH}_4\text{OH}$ . The speed of precipitation will affect physicochemical properties of the product, including particle size, morphology, and crystal structure, which further impact photocatalytic activity.

## 2. Materials and Methods

### 2.1 Materials

Materials used in this research were  $\text{Bi}(\text{NO}_3)_3 \cdot 5\text{H}_2\text{O}$  bought from Sigma Aldrich, Singapore;  $\text{HNO}_3$  65%; NaOH;  $\text{NH}_4\text{OH}$ ; methyl orange bought from Merck, Darmstadt, Germany; and distilled water.

### 2.2 Synthesis of bismuth oxide

Precursor solution containing a mixture of 10 g of  $\text{Bi}(\text{NO}_3)_3 \cdot 5\text{H}_2\text{O}$  and 20 ml of  $\text{HNO}_3$  65% was stirred (Cimarec SP131320-33Q) at 600 rpm.  $\text{NH}_4\text{OH}$  25% was then added with constant stirring, continued for another 1 h, until the precipitate was formed and pH 9-10 was achieved. The

precipitate was then separated by filtration using a filter paper, washed with distilled water several times, and dried in an oven (Isotemp 630 F) at 110 °C for 24 h. The dried powder was heated at 500 °C for 1 h in a furnace (Eurotherm 2116, Worthing, UK). The same procedure was conducted to synthesize bismuth oxide with the alternative precipitating agent, NaOH 25%. Further, the sample types are labeled with BO1, BO2, BO3, or BO4 to indicate in this order a product synthesized using  $\text{NH}_4\text{OH}$  before calcination, product synthesized using NaOH before calcination, product synthesized using  $\text{NH}_4\text{OH}$  after calcination, or product synthesized using NaOH after calcination.

### 2.3 Characterization

The  $\text{Bi}_2\text{O}_3$  particles' crystal structures were characterized using XRD (Shimadzu,  $\text{CuK}\alpha$  radiation source, 30 kV voltage, 30 mA electric current, X-Ray radiation wavelength 1.54178 Å, and range of  $2\theta$   $10^\circ$ - $90^\circ$ ), and scan speed of 2 deg  $\text{min}^{-1}$ . The morphology of the  $\text{Bi}_2\text{O}_3$  was imaged by SEM (JEOL-JSM- 6510LV, voltage 30 KV). The presence of functional groups on the surfaces of  $\text{Bi}_2\text{O}_3$  was determined by FTIR (Bruker, scanning over 500-4250  $\text{cm}^{-1}$ ) with attenuated total reflection (ATR) technique. DRS-UV (UV 1700 Pharmaspec) was applied to determine the band gaps. Meanwhile, thermal stability of the product before calcination was analysed using TGA (LINSEIS STA Platinum Series, temperature range 0-800 °C, heat flow 0-140 mW). Approximately 23 mg of BO1 sample was heated at a heating rate of 3 °C/min from room temperature to 900 °C in air environment. The gas flow rate was kept at 60 ml/min.

### 2.4 Photocatalytic activity test

The photocatalytic test was performed in a photocatalysis reactor (Figure 1). 0.1 g of bismuth oxide was added into 50 ml of methyl orange solution (5 ppm) as pollutant model and then stirred at 600 rpm with a magnetic stirrer. The exposure times were 2, 4, 6, 8, and 10 hours. The irradiation was from a 65 watt tungsten lamp. In order to evaluate the adsorption effect, the sample had been also left in the dark for 2 hours. The concentration of methyl orange degraded by bismuth oxide was measured by UV-Vis spectrophotometer (Genesys 105) at wavelength of 463 nm (Astuti *et al.*, 2016, 2017).

## 3. Results and Discussion

### 3.1. Physical and chemical properties of bismuth oxide affected by precipitating agent

The bismuth oxide powders after drying were both white when prepared with  $\text{NH}_4\text{OH}$  or NaOH precipitating

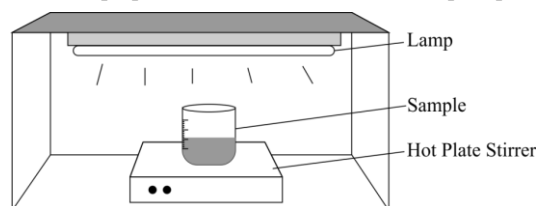
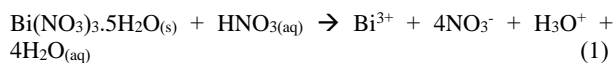
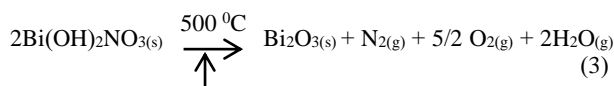
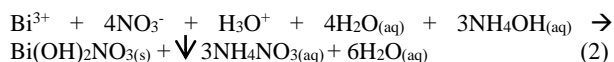


Figure 1. The photocatalytic reactor

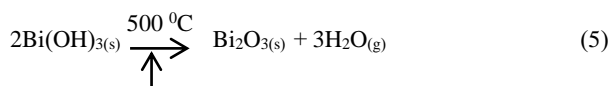
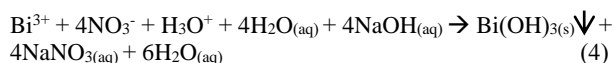
agents, as shown in Figures 2a and b. The color of the powder turned bright yellow or pale yellow after calcination at 500 °C for 1 h, for samples prepared with NH<sub>4</sub>OH and NaOH, respectively, as shown in Figures 2c and d. The proposed reaction scheme for the bismuth oxide synthesis with bismuth nitrate pentahydrate precursor is as follows:



The reactions proposed after addition of NH<sub>4</sub>OH are:



while the reactions proposed with NaOH are as follows:



These proposed mechanisms are based on the common reaction discussed in Vogel (1961).

TG and DTG analyses were conducted to observe the decomposition steps and BO1 was used as a representative sample. Figure 3 shows the decomposition of Bi(OH)<sub>2</sub>NO<sub>3</sub> compound (product of reaction between bismuth nitrate pentahydrate, HNO<sub>3</sub> and NH<sub>4</sub>OH, see reactions no. (1) and (2)) in the calcination process from room temperature to 900 °C with heating rate of 3°C per minute. The weight loss of around 2% from room temperature to 130 °C was due to the evaporation of water and NH<sub>4</sub>OH (La *et al.*, 2013). Maximum weight loss of around 53.82% occurred at 240-310 °C owing to decomposition of hydroxide and nitrite from Bi(OH)<sub>2</sub>NO<sub>3</sub> and NH<sub>4</sub>NO<sub>3</sub> as shown in reaction (2) (Acharya, Subbaiah, Anand, & Das, 2003; Chaturvedi & Dave, 2013), and by 450 °C there was a slight weight loss (9.53%) (Sharma, Diwan, & Pandey, 2019). At 450-550 °C, the weight decreased by 3.5% due to further decomposition of impurities and formation of α-Bi<sub>2</sub>O<sub>3</sub> (Salazar-Pérez *et al.*, 2005). The slow decomposition rate from 310 °C to 550 °C is due to the formation of an intermediate compound before Bi<sub>2</sub>O<sub>3</sub> was produced (Levin & Roth, 1964; Sharma *et al.*, 2019). Moreover, there is no considerable weight decrease after 550 °C, demonstrating that the remaining sample was Bi<sub>2</sub>O<sub>3</sub> for about 30.82% by weight.

The presence of Bi<sub>2</sub>O<sub>3</sub> and impurities were observed on the as-prepared and after calcination products in their FTIR spectra, shown in Figure 4. All of the four samples (i.e. BO1, BO2, BO3, BO4) contained -OH and N-O functional groups, shown by vibration modes at 3400 and 1300 cm<sup>-1</sup>, respectively. Vibrations at 400-800 cm<sup>-1</sup> were also observed for all samples indicating that Bi-O was formed as a fingerprint of the Bi metal (Abdullah, Abdullah, Zainal, Hussein, & Ban, 2012). However, the intensities of those functional groups (-OH and NO) differed by sample type.



Figure 2. The products after drying in an oven for 24 hours at 110 °C, precipitated using (a) NH<sub>4</sub>OH (BO1) or (b) NaOH (BO2); calcination of products (a) and (b) at 500 °C for 1 hour in a furnace generated (c) a bright yellow (BO3) and (d) yellow pale powder (BO4), respectively

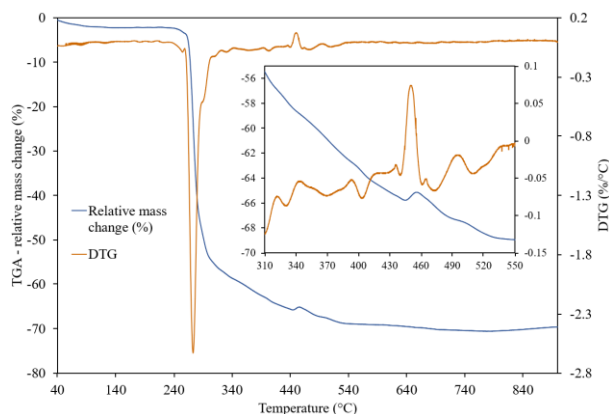


Figure 3. Thermogravimetric and differential thermogravimetric analysis (TGA-DTG) of product synthesized using NH<sub>4</sub>OH as precipitating agent and heated at 110 °C for 1 hour

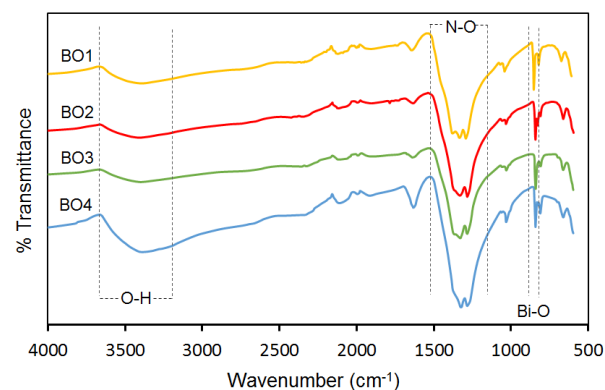


Figure 4. FTIR spectra of products before and after calcination

The contents of OH and NO functional groups in all products before and after calcination (BO1, BO2, BO3 and BO4) can be estimated from absorbances at wavenumbers of

about  $3400\text{ cm}^{-1}$  and  $1300\text{ cm}^{-1}$ , respectively, using also a constant wavenumber of about  $1600\text{ cm}^{-1}$  for each sample. Based on Table 1, it can be seen that the absorbances by both these functional groups were decreased by calcination. This indicates that the levels of OH and NO declined during calcination, according to Lambert-Beer law of absorbance being directly proportional to the amount of the analyte.

Table 1 also shows that the absorbances of peaks attributed to OH and NO functional groups in BO4 were slightly decreased by calcination. However, the decrease in BO3 was greater than that in BO4. This indicates that the purity of bismuth oxide synthesized using  $\text{NH}_4\text{OH}$  was higher, since the presence of other substances, such as OH and NO, decreased during calcination. This deduction is supported by other research on bismuth oxide synthesized using  $\text{NH}_4\text{OH}$  as precipitating agent, conducted by Patil *et al.* (2005), (Hwang *et al.*, 2009), and Bogusz *et al.* (2014).

Table 1. Comparison of absorbances by O-H and N-O functional groups in products prepared with  $\text{NH}_4\text{OH}$  or NaOH as the precipitating agent, with control absorbance at  $1633\text{ cm}^{-1}$

Treatments	Type of functional group	Absorbance ratio	
		$\text{NH}_4\text{OH}$ as precipitating agent	NaOH as precipitating agent
Drying with oven	O-H	3.737	2.591
	N-O	9.842	2.864
Calcination	O-H	1.896	2.045
	N-O	3.384	2.313

### 3.2. Structural and morphological characteristics

Figure 5 shows X-ray diffractograms of the bismuth oxides. The crystalline structure of bismuth oxide synthesized using a weak base ( $\text{NH}_4\text{OH}$ ) was a mixture of bismuth oxides with a monoclinic ( $\alpha\text{-Bi}_2\text{O}_3$ ; JCPDS no 76-1730) and a tetragonal crystal structure ( $\beta\text{-Bi}_2\text{O}_3$ ; JCPDS no 74-1374). The highest peaks of  $\alpha\text{-Bi}_2\text{O}_3$  and  $\beta\text{-Bi}_2\text{O}_3$  were found at  $2\theta$  of 27.38, 33.25, and 46.39 degrees and at 27.99, 33.75, and 55.59 degrees, respectively, as shown in Figure 5a. Meanwhile, the use of the strong base NaOH as the precipitating agent produced bismuth oxide with a mixture of monoclinic ( $\alpha\text{-Bi}_2\text{O}_3$ ; JCPDS no 72-0398), tetragonal ( $\beta\text{-Bi}_2\text{O}_3$ ; JCPDS no 76-0147) and face-centered cubic ( $\delta\text{-Bi}_2\text{O}_3$ ; JCPDS no 74-1633) crystallites, as shown in Figure 5b. The peaks of  $\alpha\text{-Bi}_2\text{O}_3$ ,  $\beta\text{-Bi}_2\text{O}_3$  and  $\delta\text{-Bi}_2\text{O}_3$  were found at  $2\theta$  of 21.82, 33.35 and 46.49; 16.19, 32.71, and 57.43; and 31.56, 45.24 and 65.90 degrees, respectively.

A report by Hernandez-Delgadillo *et al.* (2013) on the synthesis of bismuth oxide by precipitation, using  $\text{NH}_4\text{OH}$  as precipitating agent and  $\text{Bi}(\text{NO}_3)_3 \cdot 5\text{H}_2\text{O}$  as precursor, showed that the product based on the XRD data was  $\alpha\text{-Bi}_2\text{O}_3$ ; meanwhile Bartonickova *et al.* (2007) reported that using the same raw material and precipitating agent produced  $\alpha\text{-Bi}_2\text{O}_3$  and  $\beta\text{-Bi}_2\text{O}_3$ , which is in agreement with our result. The synthesis using NaOH gave  $\alpha\text{-Bi}_2\text{O}_3$ ,  $\beta\text{-Bi}_2\text{O}_3$  and  $\delta\text{-Bi}_2\text{O}_3$ ; however, no one has reported on the use of this strong base as the precipitating agent in the bismuth oxide formation, so as we cannot compare our result to prior literature.

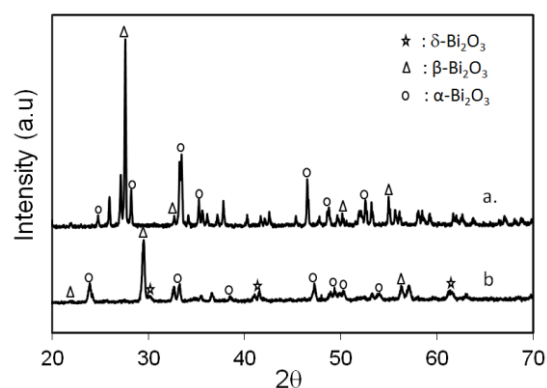


Figure 5. X-Ray diffractograms of (a) BO3, and (b) BO4

Figure 6 shows the morphology of bismuth oxides synthesized using both the weak (Figure 6a) and the strong base (Figure 6b) as irregular-shaped flat plates with particle sizes of 0.6-5.2  $\mu\text{m}$  and 2.5-10  $\mu\text{m}$ , respectively. The different particle sizes of the products might be due to the role of weak and strong bases on precipitation. During precipitation, a weak base tended to react slowly with the bismuth (III) ions, and therefore, the nucleation and growth of the particles was also slow. On the other hand, a comparatively fast reaction might occur during precipitation with a strong base, with consequently larger particles generated by fast nucleation and growth of the crystals.

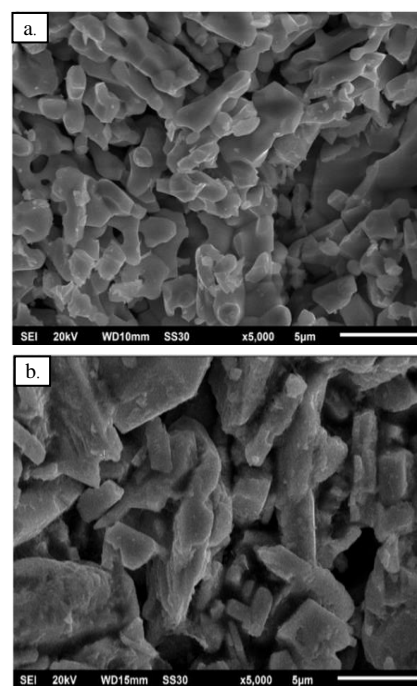


Figure 6. SEM images of (a) BO3, and (b) BO4

### 3.3 Photocatalytic activity test of bismuth oxide

The photocatalytic activity of bismuth oxide was quantified by observing the degradation of methyl orange as

an organic pollutant. The degradation was tested for 2, 4, 6, 8 and 10 hours under visible light irradiation (65 Watt tungsten lamp). The concentration of non-degraded methyl orange was then determined by UV-Vis spectrophotometer at a wavelength of 463 nm. The methyl orange degradation was calculated as follows:

$$\% \text{ Degradation} = \frac{C_0 - C}{C_0} \times 100\%$$

$C_0$  = initial concentration,  $C$  = concentration of methyl orange after degradation

The photocatalytic activities of bismuth oxides synthesized with two alternative precipitating agents are presented in Figure 7. It shows that methyl orange degradation by bismuth oxide increased with exposure time to visible light irradiation. The methyl orange degradations by BO3 and BO4 after 2 hours without visible light irradiation were 2.98% and 1.56%; whereas the percentages of methyl orange degradation by BO3 for 2, 4, 6, 8 and 10 hours of visible light irradiation were 15.78%; 36.82%; 50.80%; 65.70% and 76.14%, respectively. The methyl orange degradations by bismuth oxide synthesized using NaOH precipitating agent (BO4) were for these exposures 4.80%, 16.82%, 38.12%, 45.44% and 50.66%. The higher photocatalytic activity of BO3 is caused by the difference in bandgap energy. As seen in Figure 8, BO3 has 2.88 eV and 2.51 eV assigned to  $\alpha$ -Bi<sub>2</sub>O<sub>3</sub> and  $\beta$ -Bi<sub>2</sub>O<sub>3</sub>, respectively; while the bandgap of BO4 was only 2.80 eV attributed to  $\alpha$ -Bi<sub>2</sub>O<sub>3</sub>. It has been reported that a combination of  $\alpha$ -Bi<sub>2</sub>O<sub>3</sub> and  $\beta$ -Bi<sub>2</sub>O<sub>3</sub> significantly increases the photocatalytic activity of bismuth oxide (Hou *et al.*, 2013). Furthermore, the particle size of BO3 is smaller than that of BO4 as confirmed by SEM images in Figure 6, so that it also has the larger specific surface area. Sample in the form of a powder with a large surface area will have enhanced photocatalytic activity: the larger specific surface area allows more dye molecules (methyl orange) to be absorbed onto the surfaces of photocatalyst.

The results of this study are slightly different from those reported by Iyyapushpam, Nishanthi, and Pathinettam Padiyan (2013), where the photocatalytic activity test of 0.1 g  $\beta$ -Bi<sub>2</sub>O<sub>3</sub> added into 16.4 ppm methyl orange, after visible light irradiation for 240 minutes, showed 85% degradation of methyl orange. The lesser degradation in our investigation could be due to impure products, as the bismuth oxide was a mixture of  $\alpha$ -Bi<sub>2</sub>O<sub>3</sub>,  $\beta$ -Bi<sub>2</sub>O<sub>3</sub> and  $\delta$ -Bi<sub>2</sub>O<sub>3</sub> according to the X-ray diffractogram (Figure 5). In addition, the remaining OH and NO functional groups in the samples, confirmed by FTIR spectra (Figure 4), might also reduce the photocatalytic activity.

According to Liu, Deng, Yao, Jiang, and Shen (2015), photocatalytic activity of bismuth oxide for methyl orange degradation can be used to determine the degradation rate through chemical kinetics; in general, the photocatalysis reaction has first-order kinetics. The rate constant can then be determined from:

$$\ln C_t = \ln C_0 + kt$$

where  $C_t$  is concentration of dye (ppm) at time  $t$ ,  $C_0$  is concentration of dye molecule (ppm) at time  $t_0$  and  $k$  is the rate constant of degradation ( $s^{-1}$ ). The first order kinetics of

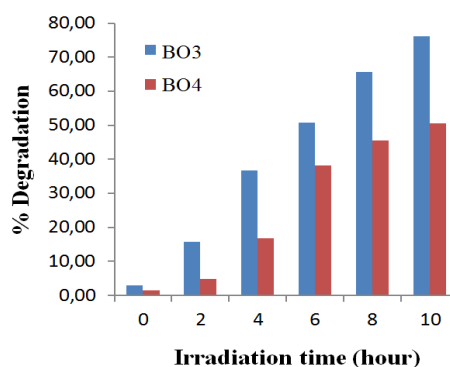


Figure 7. Percentage of methyl orange degradation by bismuth oxide synthesized using the two alternative precipitating agents

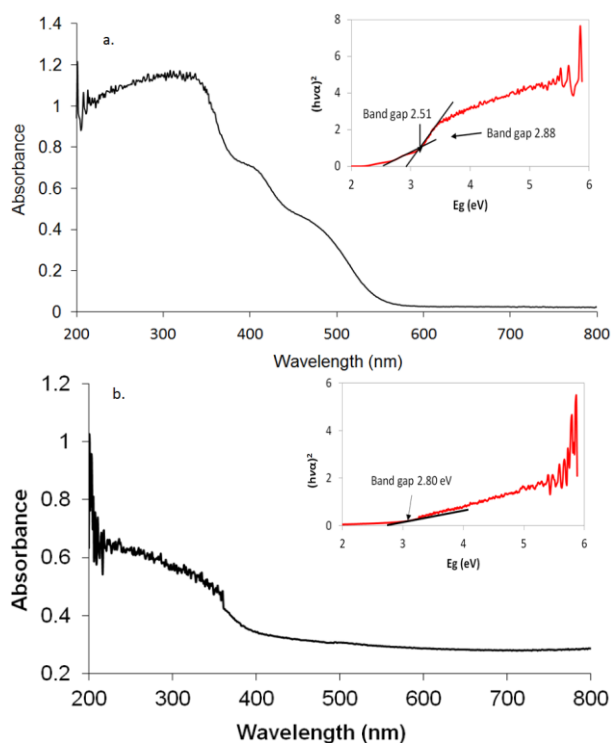


Figure 8. Diffuse reflectance spectrum and Tauc Plot transformed reflectance spectrum (inset) of (a) BO3, and (b) BO4

methyl orange degradation by bismuth oxide are presented in Figure 9 by plotting  $\ln C_t$  vs  $t$ . The degradation rate constants for the two types of samples are  $2.38 \times 10^{-5} s^{-1}$ , and  $0.68 \times 10^{-5} s^{-1}$ , for  $k_{NH_4OH}$  and  $k_{NaOH}$ . These results indicate that the bismuth oxide photocatalyst synthesized with  $NH_4OH$  has better photocatalytic activity than that synthesized with  $NaOH$ . The higher the rate constant ( $k$ ) of degradation, the higher is the photocatalytic activity of the photocatalyst.

#### 4. Conclusions

The use of different precipitating agents in synthesis of bismuth oxide by precipitation affects the characteristics of the obtained product. In this study, weak and strong bases

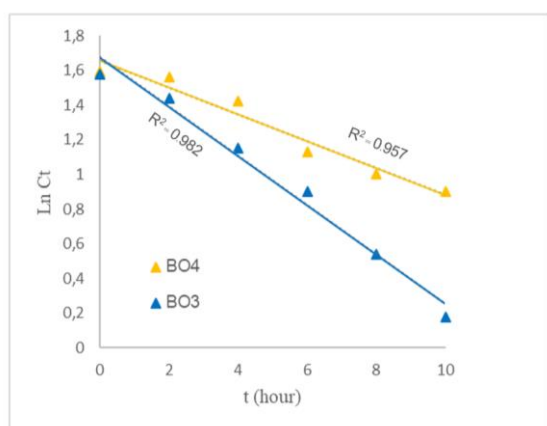


Figure 9. First-order kinetics of methyl orange degradation by  $\text{NH}_4\text{OH}$ -bismuth oxide and  $\text{NaOH}$ -bismuth oxide

were used as alternative precipitating agents in bismuth oxide synthesis by precipitation. The results showed that the use of a weak base ( $\text{NH}_4\text{OH}$ ) as precipitating agent produced better physicochemical properties and photocatalytic activity of bismuth oxide than using the strong base  $\text{NaOH}$ . The former had fewer polymorphic components in the product ( $\alpha$ - and  $\beta$ - $\text{Bi}_2\text{O}_3$ ), smaller particle sizes (0.6-5.2  $\mu\text{m}$ ) and better photocatalytic activity with a higher reaction rate constant ( $2.38 \times 10^{-5} \text{ s}^{-1}$ ). The use of the strong base  $\text{NaOH}$  generated more  $\text{OH}^-$  ions, because it dissociates perfectly in water, while the weak base  $\text{NH}_4\text{OH}$  produces fewer  $\text{OH}^-$  ions by partial dissociation. Therefore, in order to precipitate  $\text{Bi}^{3+}$  ions,  $\text{NaOH}$  as the precipitating agent acts faster than  $\text{NH}_4\text{OH}$ . The fast or slow precipitation choice will affect physicochemical properties, and these impact in turn the photocatalytic activity.

### Acknowledgements

The author would like to thank Diponegoro University for financial support with the grant no. 831.1-05/UN7.P4.3/PP/2017 through Riset Publikasi Internasional (RPI) 2017 and also Postdoctoral program in 2017 conducted in Hiroshima University, Japan. Furthermore, Yayuk Astuti would like to thank Prof. Jo Da Costa from Queensland University, Australia and Dr. G. Bhaduri from Manipal University Jaipur, India for their valuable comments on this manuscript.

### References

- Abdullah, E. A., Abdullah, A. H., Zainal, Z., Hussein, M. Z., & Ban, T. K. (2012). Synthesis and characterisation of penta-bismuth hepta-oxide nitrate,  $\text{Bi}_5\text{O}_7\text{NO}_3$ , as a new adsorbent for methyl orange removal from an aqueous solution. *Journal of Chemistry*, 9(4), 2429-2438.
- Acharya, R., Subbaiah, T., Anand, S., & Das, R. (2003). Effect of precipitating agents on the physico chemical and electrolytic characteristics of nickel hydroxide. *Materials Letters*, 57(20), 3089-3095.
- Aruna, S. T., & Mukasyan, A. S. (2008). Combustion synthesis and nanomaterials. *Current Opinion in Solid State and Materials Science*, 12(3), 44-50.

- Astuti, Y., Arnelli, Pardoyo, Fauziyah, A., Nurhayati, S., Wulansari, A. D., Bhaduri, G. A. (2017). Studying impact of different precipitating agents on crystal structure, morphology and photocatalytic activity of bismuth oxide. *Bulletin of Chemical Reaction Engineering and Catalysis*, 12(3), 478-484.
- Astuti, Y., Fauziyah, A., Nurhayati, S., Wulansari, A. D., Andianingrum, R., Hakim, A. R., & Bhaduri, G. (2016). Synthesis of  $\alpha$ -Bismuth oxide using solution combustion method and its photocatalytic properties. *IOP Conference Series: Materials Science and Engineering*, 107, 1-7.
- Astuti, Y., Ningsih, H., Arneli, & Darmawan, A. (2018). Influence of  $\text{NH}_4\text{OH}$  concentration in synthesis of bismuth oxide to physicochemical properties and photocatalytic activity in methyl orange degradation. *AIP Conference Proceedings*, 2026, 020002-1-6.
- Bartoniczkova, E., Cihlar, J., & Castkova, K. (2007). Microwave-assisted synthesis of bismuth oxide. *Processing and Application of Ceramics*, 1(1-2), 29-33.
- Bogusz, K., Tehei, M., Stewart, C., McDonald, M., Cardillo, D., Lerch, M., Konstantinov, K. (2014). Synthesis of potential theranostic system consisting of methotrexate-immobilized (3-aminopropyl) tri methoxysilane coated  $\alpha$ - $\text{Bi}_2\text{O}_3$  nanoparticles for cancer treatment. *RSC Advances*, 4(46), 24412-24419.
- Boivin, J.-C. (2001). Structural and electrochemical features of fast oxide ion conductors. *International Journal of Inorganic Materials*, 3(8), 1261-1266.
- Cao, G. (2004). *Nanostructures and nanomaterials: Synthesis, properties and applications*. Singapore: World Scientific.
- Chaturvedi, S., & Dave, P. N. (2013). Review on thermal decomposition of ammonium nitrate. *Journal of Energetic Materials*, 31(1), 1-26.
- Goodenough, J. B. (2003). Oxide-ion electrolytes. *Annual Review of Materials Research*, 33(1), 91-128.
- Hernandez-Delgadillo, R., Velasco-Arias, D., Martinez-Sanmiguel, J. J., Diaz, D., Zumeta-Dube, I., Arevalo-Niño, K., & Cabral-Romero, C. (2013). Bismuth oxide aqueous colloidal nanoparticles inhibit *Candida albicans* growth and biofilm formation. *International Journal of Nanomedicine*, 8, 1645-1652.
- Hou, J., Yang, C., Wang, Z., Zhou, W., Jiao, S., & Zhu, H. (2013). In situ synthesis of  $\alpha$ - $\beta$  phase heterojunction on  $\text{Bi}_2\text{O}_3$  nanowires with exceptional visible-light photocatalytic performance. *Applied Catalysis B: Environmental*, 142, 504-511.
- Hwang, G. H., Han, W. K., Kim, S. J., Hong, S. J., Park, J. S., Park, H. J., & Kang, S. G. (2009). An electrochemical preparation of bismuth nanoparticles by reduction of bismuth oxide nanoparticles and their application as an environmental sensor. *Journal of Ceramic Processing Research*, 10(2), 190-194.
- Iyyapushpam, S., Nishanthi, S. T., & Pathinettam Padiyan, D. (2013). Degradation of methyl orange using bismuth oxide. *Proceedings of the International Conference on "Advanced Nanomaterials and Emerging*

- Engineering Technologies", ICANMEET 2013.*
- Kharton, V. V., Naumovich, E. N., Yaremchenko, A. A., & Marques, F. M. (2001). Research on the electrochemistry of oxygen ion conductors in the former Soviet Union. *Journal of Solid State Electrochemistry*, 5(3), 160-187.
- La, J., Huang, Y., Luo, G., Lai, J., Liu, C., & Chu, G. (2013). Synthesis of bismuth oxide nanoparticles by solution combustion method. *Particulate Science and Technology*, 31(3), 287-290.
- Levin, E. M., & Roth, R. S. (1964). Polymorphism of bismuth sesquioxide. I. Pure Bi<sub>2</sub>O<sub>3</sub>. *Journal of Research of the National Bureau of Standards. Section A, Physics and Chemistry*, 68(2), 189.
- Li, W. (2006). Facile synthesis of monodisperse Bi<sub>2</sub>O<sub>3</sub> nanoparticles. *Materials Chemistry and Physics*, 99(1), 174-180.
- Liu, X., Deng, H., Yao, W., Jiang, Q., & Shen, J. (2015). Preparation and photocatalytic activity of Y-doped Bi<sub>2</sub>O<sub>3</sub>. *Journal of Alloys and Compounds*, 651, 135-142.
- Mallahi, M., Shokuhfar, A., Vaezi, M., Esmailirad, A., & Mazinani, V. (2014). Synthesis and characterization of bismuth oxide nanoparticles via sol-gel method. *American Journal of Engineering Research*, 3, 162-165.
- Patil, M., Deshpande, V., Dhage, S., & Ravi, V. (2005). Synthesis of bismuth oxide nanoparticles at 100 C. *Materials letters*, 59(19-20), 2523-2525.
- Salazar-Pérez, A., Camacho-López, M., Morales-Luckie, R., Sánchez-Mendieta, V., Ureña-Núñez, F., & Arenas-Alatorre, J. (2005). Structural evolution of Bi<sub>2</sub>O<sub>3</sub> prepared by thermal oxidation of bismuth nanoparticles. *Superficies y vacío*, 18(3), 4-8.
- Sammes, N., Tompsett, G., Näfe, H., & Aldinger, F. (1999). Bismuth based oxide electrolytes—structure and ionic conductivity. *Journal of the European Ceramic Society*, 19(10), 1801-1826.
- Serpone, N., & Pelizzetti, E. (1989). *Photocatalysis, fundamentals and applications*. New York, NY: Wiley.
- Sharma, P., Diwan, P., & Pandey, O. (2019). Impact of environment on the kinetics involved in the solid-state synthesis of bismuth ferrite. *Materials Chemistry and Physics*, 233, 171-179.
- Skoog, D. A., West, D. M., Holler, F. J., & Crouch, S. (2013). *Fundamentals of analytical chemistry*. Toronto, Canada, Nelson Education.
- Stewart, C., Konstantinov, K., McKinnon, S., Guatelli, S., Lerch, M., Rosenfeld, A., . . . Corde, S. (2016). First proof of bismuth oxide nanoparticles as efficient radiosensitisers on highly radioresistant cancer cells. *Physica Medica*, 32(11), 1444-1452.
- Switzer, J. A., Shumsky, M. G., & Bohannon, E. W. (1999). Electrodeposited ceramic single crystals. *Science*, 284(5412), 293-296.
- Vogel, A. I. (1961). *Text-book of quantitative inorganic analysis including elementary instrumental analysis*. New York, NY: Longman.
- Wu, C., Shen, L., Huang, Q., & Zhang, Y. C. (2011). Hydrothermal synthesis and characterization of Bi<sub>2</sub>O<sub>3</sub> nanowires. *Materials Letters*, 65(7), 1134-1136.